Revista Brasileira de Ciência do Solo

Division - Soil Processes and Properties | Commission – Soil Physics

Soil hydraulic properties, mineralogical alteration and pore formation in Regosols from southern Brazil

Fabrício de Araújo Pedron[(1)*], Gabriel Antônio Deobald[(2)], Paulo Ivonir Gubiani[(1)], Luís Antônio Coutrim dos Santos[(3)], Antônio Carlos de Azevedo[(4)], José Miguel Reichert[(1)] and Alice Prates Bisso Dambroz[(1)]

[(1)] Universidade Federal de Santa Maria, Departamento de Solos, Santa Maria, Rio Grande do Sul, Brasil.
[(2)] Empresa de Pesquisa Agropecuária e Extensão Rural de Santa Catarina, Florianópolis, Santa Catarina, Brasil.
[(3)] Universidade do Estado do Amazonas, Itacoatiara, Amazonas, Brasil.
[(4)] Universidade de São Paulo, Departamento de Ciência do Solo, Piracicaba, São Paulo, Brasil.

*** Corresponding author:**
E-mail: fapedron@ufsm.br

Received: January 25, 2024

Approved: April 08, 2024

How to cite: Pedron FA, Deobald GA, Gubiani PI, Santos LAC, Azevedo AC, Reichert JM, Dambroz APB. Soil hydraulic properties, mineralogical alteration and pore formation in Regosols from southern Brazil. Rev Bras Cienc Solo. 2024;48:e0240013.
https://doi.org/10.36783/18069657rbcs20240013

Editors: Reinaldo Bertola Cantarutti and João Tavares Filho.

ABSTRACT: Regosols (*Neossolos*) are soils with use limitations mainly related to effective depth, abundant presence of rock and saprolite fragments, and frequently high slope gradients; besides that, they represent a new agricultural frontier for grain production in southern Brazil. This study evaluated soil saturated hydraulic conductivity (K_{sat}) and water retention and availability in Regosols and saprolites derived from volcanic rocks in southern Brazil and the relationship of these variables with porosity in saprolithic horizons characterized by mineralogical weathering. The study was carried out on eight profiles derived from basic and acidic volcanic rocks of the Serra Geral Formation. We evaluated soil morphology, granulometry, porosity, bulk density (BD), K_{sat}, water retention, electronic/ optical microscopy and chemical composition of parent materials, and soil mineralogy. Soil K_{sat} ranged from 0.0 to 6.40 cm h^{-1} in the evaluated horizons, without significant difference between the A and Cr horizons. Seven soil profiles showed BD equal to or less than 1.28 Mg m^{-3} for the Cr samples. Total porosity in the Cr horizons was above 0.5 m^3 m^{-3} and not significantly different from A horizons. In five of the eight soil profiles, one or more Cr horizons presented greater available water than A horizons. Electronic and optical microscopy evidenced abundant cracks and mineralogical weathering in the rock samples. X-rays diffraction data also indicated advanced degree of weathering of Cr horizons, evidencing abundant formation of pores in the saprolite. and justifying the high-water retention in Regosols profiles in southern Brazil.

Keywords: weathering, regolith, rock fragments, porosity, stony soils.

INTRODUCTION

Neossolos Regolíticos (saprolithic Regosols), in the Brazilian Soil Classification System, are soils without a diagnostic B horizon, with a lithic contact below 0.50 m in depth and a Cr horizon consisting of saprolite (Santos et al., 2018a). Saprolite is defined as autochthonous geogenic material with varying degrees of weathering, but maintaining the original structure of the parent rock, which can be cut with a shovel (Pedron et al., 2009, 2015). Several studies highlight thatsaprolite in less developed soils plays important environmental and agricultural functions (Pedron et al., 2009; Santos et al., 2017), although we are still seeking a better understanding of the saprolite effects in soil water dynamics and plant development (Pereira et al., 2023; Fachi et al., 2023).

In the volcanic plateau of southern Brazil, more than 25 % of the area consists of shallow (less than 0.50 m) and moderately deep (0.50 m to less than 1.00 m), with saprolite occurring within 1.00 m from the surface. Most of these areas, especially those where saprolithic Regosols predominate, are considered inappropriate for annual grain cultivation, and should be reserved for perennial crops or environmental preservation (Streck et al., 2018). However, with the price increase of soybeans in the international market in recent years, these areas have been under strong use pressure, becoming a recent agricultural frontier in southern Brazil. This fact has promoted the indiscriminate use of shallow, stony, and steep soils, resulting in environmental degradation and ecological losses. These problems may intensify due to climate changes caused by global warming, which have increased the risk of drought in southern Brazil and may further limit the use of these soils. Therefore, a more detailed knowledge of its capabilities and limitations is necessary for sustainable use planning.

Low retention capacity and water availability in shallow soils stand out as a strong limiting factor for agricultural cultivation, especially in regions with little or erratic precipitation in the growing seasons. However, fragmented saprolites allow the deepening of roots in the Cr horizons, where plants can mine extra water to fulfill the demand for proper growth (Pedron et al., 2009; 2011). Field observations confirm root development in saprolite cracks (Wald et al., 2013; Pedron et al., 2015) and indicate water dynamics in these materials is related to their fracturing and cracks filling (Stürmer et al., 2009).

The Cr horizons of soils derived from sandstones may have lower, equal or even higher water retention than solum horizons (Pedron et al., 2011). Data from Pereira et al. (2023) show coarse fragments (rock and saprolite) derived from volcanic rocks can retain and release more available water for plants per unit volume than many Ferralsols, indicating saprolite also acts as a reservoir of water for plants. However, in most shallow soils that have been suffering an increase in agricultural occupation, the capabilities of saprolite to perform hydrological functions such as retaining and releasing water for plants are unknown. These functions are governed by retention and permeability properties, which are directly dependent on the saprolite porosity and soil profile weathering rate that rules the mineral alteration and pore formation (Santos et al., 2018b).

Characterization of hydraulic properties is fundamental for the proper agricultural management of shallow and stony soils and their preservation. Likewise, understanding the generation of pores by mineralogical alteration contributes to the knowledge of the behavior of these volcanic materials in southern Brazil. The main hypothesis is that alteration of vulcanic rock minerals in the saprolite horizon allows pore formation and significant water retention and availability. We evaluated soil saturated hydraulic conductivity, and water retention and availability, and contribution of mineral alteration in the saprolite horizon for pore formation in Regosols derived from volcanic rocks in southern Brazil.

MATERIALS AND METHODS

Environmental information and soil profile characterization

Eight soil profiles of *Neossolos Regolíticos* (Regosols) were selected on the volcanic Meridional Plateau edge located in the central region of the state of Rio Grande do Sul State (RS), Brazil (Figure 1). The land use for each site is presented in table 1. The climate in the study region is humid subtropical without drought, with an average annual temperature of 19.2 °C and an average annual rainfall of 1,708 mm (Maluf, 2000). The soils are derived from basic and acidic volcanic rocks of the Serra Geral Formation. Rock acidity and its chemical composition was identified using the X-Ray Fluorescence Spectrometry (FRX) technique (Buhrke et al., 1998).

Soil profiles were described and sampled according to Santos et al. (2015) and the Soil Survey Staff (2017). Cracking analysis of Cr horizons and R layers was performed according to Pedron et al. (2009), recording the angles, spacing, thickness and filling of the cracks. The weathering classes used to identify and characterize the samples of rocks and saprolites in the field followed the indication of Pedron et al. (2009, 2010).

Hydraulic analysis

Undisturbed samples were collected in metal rings with a volume of 141 cm^3 (0.06 m diameter and 0.05 m heigth) with five repetitions, in which the soil bulk density was determined according to Teixeira et al. (2017). In these samples, water retention was determined at suctions (positive value of matric potential) of 0 (effective saturation) and 0.01 MPa in a sand column (Gubiani et al., 2009). Water retention at suctions greater than 1 MPa was determined with a WP4 dew point potentiometer (Gubiani et al., 2012).

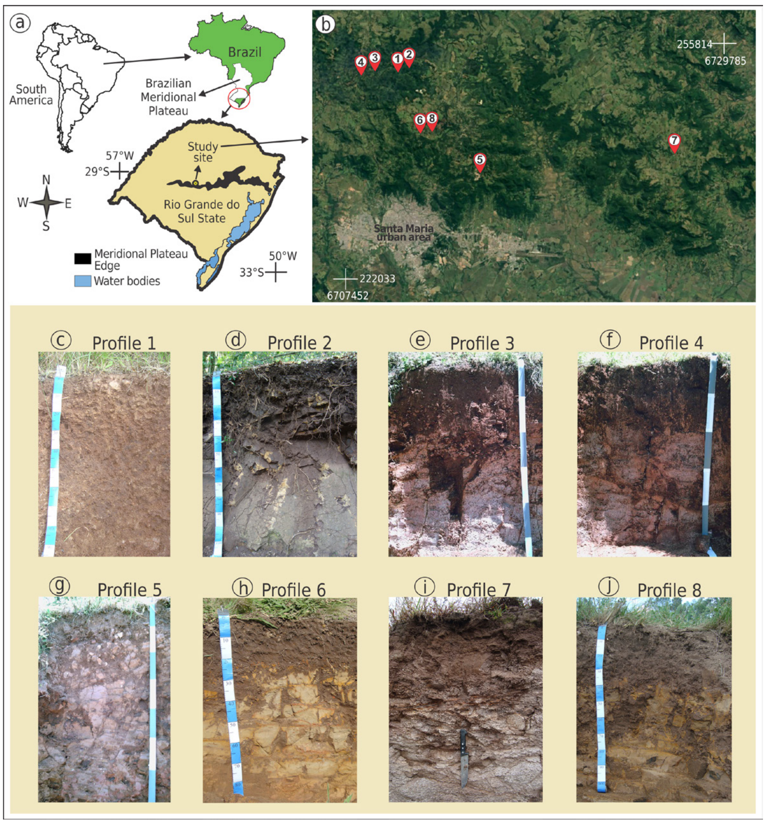

Figure 1. Location of the study area (a), with a superior view of the Meridional Plateau edge region and the distribution of sampling points (b) and the evaluated soil profiles (c to j). Satellite image taken from Google Earth® 2023. Metric scale with color segments equivalent to 0.10 m (profiles 1, 2, 3 and 8) and 0.20 m (profiles 3, 4 and 5). UTM coordinates 22J.

The available water (AW) was estimated by the water difference between the suction of 0.01 MPa (field capacity) and 1.5 MPa (permanent wilting point). The total porosity was determined by saturation of the pores (θ_{sat}) and weighing.

Saturated hydraulic conductivity (K_{sat}) was determined in undisturbed samples by the constant head permeameter method (Teixeira et al., 2017). The resistance to penetration was measured with a Stolf-type impact penetrometer (Stolf, 1991), using the Dutch equation (Equation 1).

$$R = \left(\frac{fMgh}{Ax}\right) + \left[\frac{(M+m)/g}{A}\right] \quad \text{Eq. 1}$$

in which: R is the soil resistance (usually expressed as kgf cm^{-2}, or MPa, with the approximations g = 10 m s^{-2} and 1 MPa = 10 kgf cm^{-2}); Mg is the weight of the considered mass (kgf cm^{-2}); h is the height of fall of the mass causing the impact (cm); x is the unitary penetration caused by one impact (cm/impact); (M+m) is the total mass (mass of the impact plus the mass of the equipment) in kg; g is the gravity acceleration (m s^{-2}); A is the cone base area (cm^2); and f is the kinetic energy of the impact, which is equal to M/(M+m).

Micromorphological analysis

Samples of Cr horizons were gold coated and submitted to scanning electron microscopy (SEM) equipped with backscattered electrons (BSE) and energy-dispersive X-ray (EDS) detectors (Goldstein et al., 1992). Rock fragments (RCr) with preserved structure were sampled for thin sections used in the micromorphological analysis in a petrographic polarization microscope (Murphy, 1986), where the texture, composition, size and percentage of minerals in the sample were identified.

Chemical analysis

Chemical dissolution of iron oxides via dithionite-citrate-sodium bicarbonate – DCB (Fed) of the fine earth fraction was carried out according to the procedures described by Mehra and Jackson (1960). The identification of primary and secondary minerals present in the material was carried out by X-ray diffraction (XRD) in soil samples (clay fraction) and in samples of saprolite and rock, according to Whitting and Allardice (1986). Soil organic carbon (SOC) content was determined via wet combustion with potassium dichromate 0.067 mol L^{-1} and external heating. The titration of SOC extracts was performed with 0.5 mol L^{-1} ferrous ammonium sulfate (Yeomans and Bremner, 1988).

Mineralogical analysis

Clay fraction of the soil was analyzed in an oriented slide with the following treatments: clay saturated with K^+ at room temperature (25 °C); clay saturated with K^+ and heated to 350 °C; clay saturated with K^+ and heated to 550 °C; clay saturated with Mg^{2+} at room temperature (25 °C); clay saturated with Mg^{2+} and subsequently solvated with ethylene glycol (25 °C). Saprolite and rock samples were analyzed on powdered slides. The XRD were obtained in a vertical goniometer equipped with a Ni filter and Cu Kα radiation, being operated at 20 mA and 40 kV, with an angular velocity of 0.5° 2θ min^{-1} and reading intervals of 0-65° 2θ for the samples of saprolites and rocks and 0-45° 2θ for clay samples.

Kaolinite (Kt) quantification was performed by thermal analysis, in samples of horizons A and Cr fractionated in a sieve with a 2 mm mesh, previously treated (deferrified) with DCB, evaluated in a derivatograph with a module of Thermogravimetry (TG) and Differential Thermal Analysis (DTA) simultaneously. The Kt was quantified by the mass loss in the intervals of 450 and 550 °C, considering a mass loss of 13.9 % referring to the dehydroxylation effect (Costa et al., 2004).

Table 1. Morphological and environmental data of Regosols from the Serra Geral Formation in southern Brazil

Profiles/	Horizon	Layers	SG/U[(1)]	FT[(2)]	DF[(3)]	WC[(4)]	PRPR[(5)]	Roots	Altitude
		m		mm	cm		kPa		m
P1	A	0.00-0.10	SS/ BF	nd	nd	nd	nd	Common	284
	Cr1	0.10-0.50		2	20	I6	4.90	Few	
	Cr2	0.50-0.90+		2	20	I5	3.24	Very few	
P2	A	0.00-0.10	SS/ FL	nd	nd	nd	nd	Many	235
	Cr1	0.10-0.30		2	5	I5	5.29	Common	
	Cr2	0.30-0.60		2	5	I5	8.04	Common	
	RCr	0.60-1.50+		2	5	I3	12.65	Few	
P3	A	0.00-0.23	GS/ NP	nd	nd	nd	nd	Many	228
	Cr1	0.23-0.43		5	20	I5	7.75	Common	
	Cr2	0.43-1.20		5	20	I5	6.37	Few	
	RCr	1.20-1.40+		5	20	I3	13.53	Very few	
P4	A	0.00-0.30	GS/ NP	nd	nd	nd	nd	Many	218
	Cr	0.30-1.15		5	8	I5	6.37	Few	
	RCr	1.15-1.50+		5	8	I2	15.39	Very few	
P5	A	0.00-0.14	U/ BF	nd	nd	nd	nd	Common	452
	Cr/A	0.14-0.53		1	5	I6	3.14	Few	
	Cr	0.53-1.40		1	5	I5	6.18	Very few	
	RCr	1.40-2.40+		1	5	I2	21.48	Very few	
P6	A	0.00-0.28	U/ CP	nd	nd	nd	nd	Common	467
	CrR	0.28-0.70		2	8	I3	12.06	Few	
	Cr	0.70-1.00+		2	8	I5	3.43	Very few	
P7	A	0.00-0.12	GS/ AG	nd	nd	nd	nd	Many	490
	Cr1	0.12-0.85		1	2	I6	6.47	Few	
	Cr2	0.85-1.40+		1	2	I5	7.85	Very few	
P8	A	0.00-0.25	GS/ NP	nd	nd	nd	nd	Common	458
	Cr/A	0.25-0.75		3	10	I5	4.22	Few	
	RCr1	0.75-1.05		3	10	I3	20.79	Very few	
	RCr2	1.05-1.20+		3	10	nd	nd	Very few	

[(1)] Slope gradient {SG: (GS: gently sloping, U: undulating, SS: strongly sloping)}/Land use {U: (NP: native pasture; BF: bushy field; CP: cultivated pasture; AG: annual grain crop; FL: florest)}; [(2)] fractures thickness (FT); [(3)] distance between fractures (DF); [(4)] weathering classes (WC) – I2: rock slightly weathered, I3: rock moderately weathered, I4: saprolite slightly weathered, I5: saprolite moderately weathered, I6: saprolite very weathered; [(5)] penetration resistance (PR). All saprolite samples (Cr, CrR, RCr) showed fractures filled with soil and roots. nd: not determined.

Statistical analysis

As the soil profiles location and their horizons cannot be randomly set, the non-parametric Kruskal-Wallis test was used to evaluate whether the horizons affected soil physical properties in each location. The non-parametric Nemenyi test was used as a post-hoc test. These tests were run with the KW_MC SAS macro (Elliott and Hynan, 2011).

RESULTS

Slope gradient of the study areas varied from gently sloping to strongly sloping. Current use was also diverse (Table 1). All studied profiles were classified according to the Brazilian soil classification system as *Neossolo Regolítico Eutrófico* (Santos et al., 2018a) and in the WRB (IUSS Working Group WRB, 2022) as follows: P1 - Eutric Regosols (Siltic, Saprolithic); P2 and P8 – Leptic, Eutric Regosols (Siltic, Saprolithic); P3, P4, P5 and P7 - Eutric Regosols (Loamic, Saprolithic).

Thickness of the A horizon ranged from 0.10 to 0.30 m (Table 1), with the lowest depths being associated with strongly sloping gradient. All profiles showed a Cr horizon with cracks filled with soil and roots. The volume of saprolite in the A horizons ranged from 14 to 75 % and the soil volume in the Cr horizons ranged from 1 to 37 %, with an average of 9.4 %. The volume of soil and the thickness of the cracks did not impede the penetration of roots in the Cr horizons, since roots were found in layers with only 1 % of soil and cracks of 2 mm.

Weathering classes (Pedron et al., 2009) ranged from I2 (RCr layer – little weathered rock) to I6 (Cr horizon – severely weathered saprolite). The Cr horizons showed penetration resistance from 3.14 to 12.06 kPa, while the RCr layers showed higher values, between 12.65 to 21.48 kPa.

Fraction of coarse material (>2 mm) varied from 138 to 748 g kg^{-1} in the A horizons, increasing in the Cr horizons, from 657 to 990 g kg^{-1} (Table 2). The texture of the horizons was quite variable. Clay content in the A horizon varied from 120 to 348 g kg^{-1}, while in the Cr horizon, the variation was from 53 to 429 g kg^{-1}. In some cases, such as P2 and P6, the clay contents in Cr are higher than those in the A horizon. The SOC ranged from 14.2 to 55.3 g kg^{-1} in the A horizon, reducing in all profiles in the Cr horizons. The Fed values ranged from 11.75 to 61.11 g kg^{-1} in P5 and P3, respectively, with higher values in A horizons, except in P8. The Kt contents ranged from 30 to 49 %, always decreasing in depth. The first four profiles showed SiO_2 contents in the RCr layer characteristic of basic rock, while the last four profiles were characterized as acidic rocks.

Table 2. Physical, chemical and mineralogical data of soil and saprolite samples of Regosols from the Serra Geral Formation in southern Brazil

Profiles	Horizons	Total sample		Fine earth			SOC(1)	Fed(2)	Kt(3)	Parent material
		>2 mm	<2 mm	Clay	Sand	Silt				
		g kg^{-1}							%	% SiO_2
P1	A	507	493	120	465	416	14.2	25.03	43	Basic 50.9
	Cr1	666	334	99	262	639	2.7	22.71	39	
	Cr2	980	20	108	279	613	2.6	12.39	37	
P2	A	748	252	234	273	492	55.3	23.05	45	Basic 55.5
	Cr1	881	119	247	269	484	29.8	20.94	38	
	Cr2	982	18	272	330	398	15.1	10.52	37	
P3	A	410	590	296	278	426	18.5	61.11	49	Basic 50.4
	Cr1	748	252	55	442	503	3.0	42.37	39	
	Cr2	980	20	53	552	395	2.5	23.32	37	
P4	A	331	669	251	377	372	19.0	45.62	40	Basic 50.4
	Cr	975	25	60	575	365	2.3	24.46	38	
P5	A	746	254	298	212	491	28.8	11.75	37	Acidic 68.6
	Cr/A	647	353	228	267	504	10.9	9.57	32	
	Cr	960	40	283	267	450	8.9	10.36	30	
P6	A	263	737	348	210	442	23.8	17.64	35	Acidic 70.5
	CrR	729	371	429	196	374	13.6	12.15	30	
	Cr	957	43	nd	nd	nd	8.2	11.24	31	
P7	A	345	655	211	396	393	12.0	21.02	34	Acidic 71.0
	Cr1	963	37	84	579	338	1.3	9.00	30	
	Cr2	990	10	73	500	428	1.8	10.53	32	
P8	A	138	862	280	143	577	19.3	30.37	43	Acidic 68.6
	Cr/A	687	313	221	196	583	5.4	71.57	33	

(1) SOC: Soil organic carbon; (2) Fed: Iron content extracted with DCB; (3) Kt: kaolinite; nd: not determined.

Seven profiles showed BD values equal to or less than 1.28 Mg m^{-3} in saprolite (Cr) samples. Only P7 showed higher values, reaching 1.43 Mg m^{-3} in the Cr2 horizon. The highest BD value for horizon A was verified at P8 (1.48 Mg m^{-3}), under degraded native grassland, while the lowest BD value was observed in P2 profile (0.87 Mg m^{-3}) under natural forest.

Except for P7, all profiles evaluated showed values of total porosity (θ_{sat}) in Cr horizons above 0.50 m^3 m^{-3} (Table 3). Only P6 showed significantly higher θ_{sat} values in the Cr horizons when compared to the A horizon. In the other profiles, there was no significant variation between the θ_{sat} in the solum and the saprolite. The microporosity (θ_{10}) was higher in at least one of the Cr horizons when compared to the A horizons in the following profiles: P1, P4, P5, P6, P7 and P8. Profiles 1, 2 and 5 did not show a significant difference in AW between the A and Cr horizons, however, in profiles 3, 4, 6, 7 and 8, one or more Cr horizons showed greater AW than the A horizons.

Soil K_{sat} ranged from 0.20 to 4.79 cm h^{-1} in the A horizons and from 0.0 to 6.40 cm h^{-1} in the Cr horizons. With the exception of P2, all profiles showed K_{sat} less than 1 cm h^{-1} in the Cr horizons. No profile showed a significant difference between the K_{sat} values of the A and Cr horizons.

Abundant presence of microcracks was identified in the saprolithic material of all profiles, which is illustrated in figure 2 with scanning electron microscopy data of samples from the Cr horizons of profiles 4 and 5. It was also possible to verify the weathering process

Table 3. Soil bulk density, volumetric water content at effective saturation and at a suction of 10 and 1500 kPa, estimated available water and the saturated hydraulic conductivity of Regosols from the Serra Geral Formation in southern Brazil

Profiles	Horizons	BD	θ_{sat}	θ_{10}	θ_{1500}	AW	K_{sat}
		Mg m^{-3}			m^3 m^{-3}		cm h^{-1}
P1	A	1.29 a	0.55 a	0.40 b	0.21 b	0.19 a	0.20 ab
	Cr1	1.18 a	0.57 a	0.44 ab	0.32 a	0.12 a	0.71 a
	Cr2	1.22 a	0.57 a	0.48 a	0.25 ab	0.23 a	0.04 b
P2	A	0.87 b	0.74 a	0.43 a	0.21 ab	0.22 a	4.79 ab
	Cr1	1.12 ab	0.60 ab	0.44 a	0.20 a	0.24 a	6.40 a
	Cr2	1.28 a	0.55 b	0.47 a	0.29 b	0.18 a	1.17 b
P3	A	1.02 b	0.67 a	0.39 ab	0.19 a	0.20 b	3.19 a
	Cr1	1.25 a	0.55 b	0.38 b	0.18 a	0.20 b	0.40 ab
	Cr2	1.04 b	0.58 ab	0.43 a	0.18 a	0.25 a	0.16 b
P4	A	1.23 a	0.54 a	0.34 b	0.21 a	0.12 b	nd
	Cr	1.24 a	0.53 a	0.43 a	0.17 b	0.26 a	nd
P5	A	1.01 a	0.64 a	0.45 b	0.28 a	0.17 a	2.01 a
	Cr/A	0.94 a	0.61 a	0.46 ab	0.22 b	0.24 a	0.18 ab
	Cr	1.00 a	0.61 a	0.52 a	0.26 ab	0.26 a	0.05 b
P6	A	1.36 a	0.50 b	0.42 b	0.22 ab	0.19 b	0.25 a
	Cr	1.15 b	0.57 a	0.53 a	0.30 a	0.23 ab	0.00 b
	CrR	1.16 b	0.57 a	0.51 ab	0.22 b	0.30 a	0.02 ab
P7	A	1.30 b	0.51 a	0.42 a	0.21 b	0.21 a	0.32 a
	Cr1	1.39 ab	0.47 ab	0.40 ab	0.27 a	0.13 b	0.01 b
	Cr2	1.43 a	0.46 b	0.36 b	0.21 b	0.15 ab	0.01 ab
P8	A	1.48 a	0.44 b	0.39 b	0.26 a	0.13 b	0.22 a
	Cr/A	1.26 ab	0.51 ab	0.46 ab	0.27 a	0.19 ab	0.18 a
	Cr	1.18 b	0.56 a	0.51 a	0.27 a	0.24 a	0.47 a

BD is the soil bulk density (Mg m^{-3}); θ_{sat}, θ_{10} and θ_{1500} (m^3 m^{-3}) are the volumetric water content at saturation and at a suction of 10 and 1500 kPa, respectively; AW (m^3 m^{-3}) is the estimated available water (AW = θ_{10} - θ_{1500}); K_{sat} is the saturated hydraulic conductivity (cm h^{-1}); Within each soil profile, horizons with the same letter do not differ by the non-parametric Nemenyi test at 0.05 error probability. nd: not determined.

of the primary minerals, especially on alkaline feldspars (plagioclase), as can be seen by viewing the striations resulting from the presence of Carlsbad-type twinning in figure 2c, associated with weathering surfaces with production of secondary minerals of the 2:1 type (Figure 2d), confirmed by the results from the EDS analyzes (Figures 2e and 2f).

Descriptive petrographic analysis of the thin sections of the RCr horizons of the different profiles (Table 4) confirmed the significant weathering in all samples. Iron oxides frequently fill cracks and cleavage planes due to the loss of optical characteristics of feldspars and the release of red coatings (iron oxide) by mafic minerals (pyroxenes and amphiboles). The petrographic evaluation confirmed the first four profiles as derived from basic rocks (P1: probably basalt; P2: basalt; P3: tholeitic basalt; P4: diabase). The vesicular/amygdaloidal structure found in the rocks of profiles 5, 6 and 8 indicate they are derived materials from lava flows on top of the sequences, since these structures derive from fast lava cooling.

The FRX data of the rock samples are shown in table 5. The silicon content in P7 and P8 was higher than 70 % and lower than 51 % in the other profiles. Aluminum, iron, calcium, magnesium, sodium, and manganese contents were higher in rocks from profiles 1, 3 and 4, while potassium contents were higher in profiles 7 and 8.

The XRD data are represented by two profiles of basic rocks and two of acidic rocks (Figure 3). In the profiles derived from basic rock (1 and 4), in the rock and saprolite samples, the reflections referring to quartz (4.25, 3.32 Å) show low intensity, while the reflections referring to calcium-sodic feldspars (plagioclase) show greater intensity in the positions 4.04, 3.21, 3.19 and 2.51 Å. Rock and saprolite samples from profiles 5 and 7 showed intense reflections related to quartz (4.25, 3.32, 2.45, 2.12, 1.81 and 1.54 Å) and potassium feldspars (3.77, 3.46, 3.31, 3.28, 3.23 and 2.98 Å). The high mineralogical weathering in the samples of saprolites in all profiles is clear in the suppression of most reflections related to primary minerals and in the appearance of reflections characteristic of secondary minerals such as kaolinite (4.40 Å) and mica/illite (10.26 Å).

In the clay fraction of the A horizon samples, 2:1 minerals from the vermiculite group were detected for all profiles (15.05 Å in the Mg+EG treatment), kaolinite (7.15 and 3.50 Å) and quartz (4.25, 3.32 Å). In profile 4, kaolinite is the most expressive mineral (intensity and area of reflection), while in profiles 1, 5 and 7 vermiculite (14.04 and 12.08 Å) showed greater expressiveness than kaolinite. Intermediate reflections in the region from 15 to 30° 2θ indicate the presence of remnants of primary minerals (micas and feldspars) in the clay fraction. Quartz reflections are more expressive in profiles 5 and 7, derived from acidic rocks.

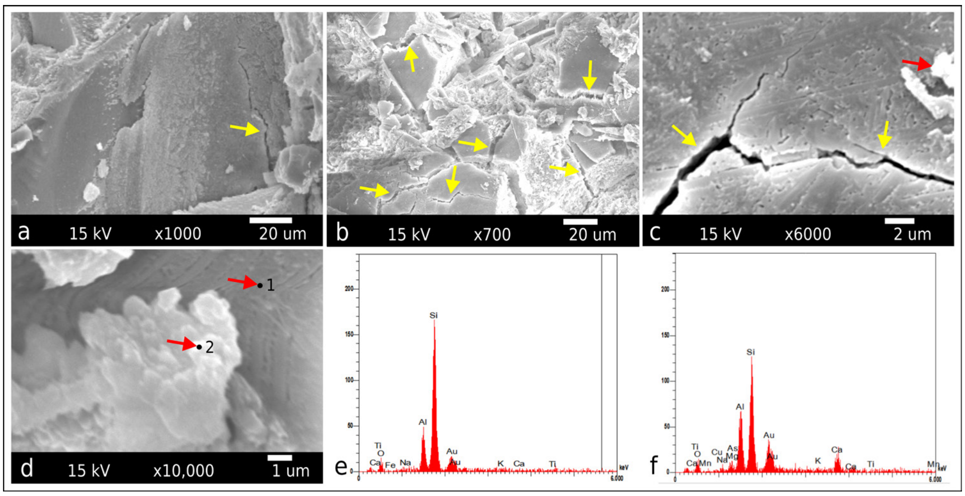

Figure 2. Micrographs obtained by scanning electron microscopy of the Cr horizons of Regosols from the Serra Geral Formation in southern Brazil (a: saprolite sample from the Cr horizon of P4; b: saprolite sample from the Cr horizon of P5; c: sample magnification in b; d: sample magnification in c with indication of the EDS analysis area (red arrow); e: EDS referring to point 1 of the sample in d; f: EDS referring to point 2 of the sample in d. Vertical and horizontal axes of e and f: intensity and keV. Yellow arrows indicate microcracks in primary minerals.

Table 4. Petrographic analysis obtained by optical microscopy of RCr samples from Regosols from the Serra Geral Formation in southern Brazil

Profiles[(1)]	Pethographic description
P1	Aphanitic rock without visible microphenocrysts and with pronounced and filled amygdaloid structures. Microgranular with microphenocrystals in the form of elongated slats of plagioclase-type feldspars, determined by the unclear presence of twins, immersed in a matrix consisting of plagioclase and mafics (pyroxenes/amphiboles). Presence of magnetite. Iron oxide is found filling fracture and cleavage planes, especially in feldspar crystals, also found in fractures of mafic minerals. High degree of alteration of the feldspars and mafics evidenced by the significant loss of the optical characteristics of the feldspars and by the release of red inks (iron oxide) by the mafics, which, together with the hazy aspect resulting from the alteration of the feldspars, prevents a precise classification of the rock. However, due to the absence of quartz, the macroscopic color, and the structures present, it can be inferred it is a basic rock.
P2	Aphanitic rock with rare microphenocrysts of feldspars and without visible structures, consisting of few elongated laths of feldspars - plagioclase type, pyroxenes and some crystals of alkaline feldspar and rare quartz, in a feldspars/pyroxenes ratio of 3:2. High amount of opaque represented by magnetite occurs. Plagioclase was recognized as being labradorite, which corresponds to a percentage of anorthite (An) between 50-70 %, showing it to be a more calcic term in the plagioclase series. Pyroxene is the augite recognized by the relief, the absence of pleochroism and the quadratic aspect established by the crossing of cleavages in section (001). Magnetite is recognized for its cubic and octahedral crystals. The degree of alteration of the rock is not accentuated, where the pyroxene shows up a little more than the feldspar, which releases reddish inks that lend a cloudy appearance to the blade. The rock is classified as a basalt-type volcanic rock.
P3	Coarse aphanitic rock, without phenocrysts, massive appearance and no visible structure. Consisting of labradorite plagioclase-type feldspar (An+50 % and -70 %) and hypersthene-type pyroxene (Mg, Fe) SiO_3 in a ratio of practically 1:1. Opaques are frequent, possibly represented by ilmenite ($FeTiO_3$), subordinately by magnetite. Quartz and biotite crystals are rare. The chemical alteration is already present, but even so, it allowed the optical recognition of the pyroxene and the type of plagioclase. Due to its petrographic characteristics, it is a volcanic rock of the tholeiitic basalt type, although texturally, it may resemble a diabase (a shallow rock, mineralogically similar to basalt).
P4	Rock with slightly more developed and strongly altered feldspar crystals, which imposes a speckled appearance, without visible structures. Consisting of plagioclase-type feldspar, varying between andesin and labradorite (Close to 50 %) and hypersthene-type pyroxene, in a ratio of 3:2. The presence of opaques, especially magnetite is greater than 5 %. Quartz presence is rare. The degree of alteration of both pyroxenes and feldspars is already significant. Along the cleavage and fracture planes of pyroxenes, oxide precipitation, possibly iron, is common. Based on its petrographic characteristics, it can be said it is a volcanic rock classified between andesite and basalt. The texture of the material suggests it is a diabase.
P5	Very fine aphanitic rock, almost glassy, without phenocrysts, presenting a vesicular/amygdaloid structure. Microscopically, the mineralogical constitution is difficult to recognize due to the fine texture and the high degree of alteration, although some blades (slats) of feldspars can be observed. In these, no twins are observed, which makes it difficult to recognize the type of feldspar, limiting the petrographic classification. The very fine texture and the vesicular/amygdaloid structure suggest this is a volcanic rock corresponding to the top of the flow.
P6 and P8	Microgranular aphanitic rock with a large amount of elongated feldspar microslats, with a layered structure and some tonsils, which indicates the position in the flow profile. Microscopically, feldspars show a rough texture in natural light when, in fact, they should be colorless, which indicates the degree of significant weathering of the rock. It is constituted by plagioclase-type feldspar identified by the unclear presence of twins, by mafics (pyroxene/amphibole) already heavily destroyed, and by magnetite, the latter recognized by its cubic and octahedral sections. The degree of alteration is significant, especially of the mafics that release reddish inks (iron oxide), which, associated with the cloudy appearance of the feldspars, makes it difficult to accurately identify the mineral constituents, consequently making it difficult to classify the rock.

[(1)] P7 was not analyzed.

DISCUSSION

Presence of roots found in cracks of saprolite horizons at depths ranging from 0.50 to 1.00 m (Table 1), although few to common for most profiles, indicates the availability of water and nutrients for plant development (Rose et al., 2003). At these depths, the saprolite identified with weathering classes I5 and I6 predominated, indicating high alteration according to Pedron et al. (2009, 2010) and affecting the BD of the horizons.

Most of the profiles showed Cr horizons with BD values equal to or less than 1.28 Mg m^{-3} (Table 3), below 1.75 Mg m^{-3}, which is the limit density for root growth of several soil textural classes suggested by Reinert et al. (2008) and Reichert et al. (2009a). Despite

Table 5. Total chemical analysis data via X-ray fluorescence of RCr samples of the Regosols from the Serra Geral Formation in southern Brazil

Elements	P1	P3	P4	P7	P6/P8
			%		
SiO_2	50.87	50.37	48.19	71.03	70.61
Al_2O_3	19.11	20.89	19.70	15.04	14.81
Fe_2O_3	17.62	10.91	8.81	5.53	6.09
CaO	4.45	10.33	9.86	1.61	0.64
K_2O	2.35	1.14	0.79	5.01	4.75
MgO	1.59	2.91	8.81	0.66	0.62
Na_2O	1.05	1.93	1.00	0.00	0.00
TiO_2	1.35	0.63	0.53	0.73	0.83
P_2O_5	0.38	0.59	1.27	0.12	1.04
MnO	0.24	0.16	0.15	0.05	0.06
Total	99.01	99.85	99.11	99.77	99.45

this, root penetration only occurred in fractures of the Cr, Cr/A, CrR and RCr horizons, as already observed by Wald et al. (2013) and Pedron et al. (2015), characterizing a paralithic material according to the Soil Survey Staff (2022). Interestingly, the BD is the main feature of the regolith used by pedologists in the field to locate the boundary between solum and saprolite (Santos et al., 2019).

Soil organic carbon and clay contents verified in the Cr horizons are predominantly found in the saprolite cracks, where clay and organic matter transported from the A horizon or recycled by the roots in the Cr itself are deposited. The filling of saprolite cracks is very common and can promote a more suitable environment for plant development, biological activity (Hasenmueller et al., 2017) and water retention, but it has also been responsible for significant reduction of soil hydraulic conductivity (Vepraskas, 2005) and water infiltration (Stürmer et al., 2009).

Low BD values for the Cr horizons are associated with a high total porosity, which varied from 0.46 to 0.61 $m^3 m^{-3}$ in all profiles (Table 3). Total porosity values are higher than those found for Regosols derived from sandstones (Pedron et al., 2011), conglomerate and granite (Pereira et al., 2023) in the same region. The micropores are the maim pores responsible for the retention of water at field capacity (Reichert et al., 2009b; Zhang et al., 2021). In six of the eight studied profiles, the field capacity was higher in at least one of the Cr compared to the A horizons (Table 3), indicating that the saprolite plays an important role in supplying water for plants.

Furthermore, the AW of evaluated soils is higher than the AW of more developed soils, such as the Ferralsols in southern Brazil (Klein et al., 2006). In five profiles (P3, P4, P6, P7 and P8), the AW was higher in the Cr horizons compared to the A horizons (Table 3), indicating the evaluated saprolites are important water reservoirs for plants, as indicated by Wald et al. (2013) and Pedron et al. (2015), to the point of being responsible for maintaining vegetation development in times of water stress (Hubbert et al., 2001). In addition to the porosity, the lack of direct interface with the atmosphere also decreases the water evaporation from Cr horizons, decreasing the fluctuation of AW during the day and the seasons.

Soil K_{sat} was less than 1 cm h^{-1} in all Cr, Cr/A and Cr/R horizons, with no significant difference when compared to A horizons. These low K_{sat} values were also found for sandstone Regosols (Pedron et al., 2011), corroborating the studies showing filling of cracks can limit the K_{sat} in these soils (Vepraskas, 2005). Soil K_{sat} is a property that presents high variability (Mesquita and Moraes, 2004) related to several factors, highlighting the continuity of pores that allow water conduction (Reichert et al., 2016, 2018; Holthusen et al., 2018).

Optical microscopy showed the weathering of primary minerals in the RCr layers in all profiles (Table 4), which can also be verified in the field with the distinction of WC I2 and I3 (Table 1). These data show, already in the first stages of alteration, the evaluated acidic and basic volcanic rocks present transformations of mafic minerals such as amphiboles and pyroxenes and feldspars potentiated by the water flow in small cracks that favor the dissolution and the beginning of the minerals disaggregation, maintaining the structural matrix of the rock and generating porosity (Wilson, 2004; Santos et al., 2018b).

All Cr samples evaluated by SEM showed abundant microcracks associated with the weathering of primary minerals, mainly feldspars (Figure 2 and 3). According to data from Navarre-Sitchler et al. (2013), for the alteration of basic volcanic rock, the porosity of the altered material increases significantly with feldspars dissolution.

The XRD data (Figure 3) clearly show the expressiveness of quartz in profiles derived from acidic rocks. The mineralogical alteration of the saprolite samples was also evident, with the transformation of primary minerals, specially feldspars into secondary minerals, such as vermiculite and kaolinite, characteristic of Regosols in southern Brazil (Pedron et al., 2012), contributing to the porosity of the saprolithic matrix (Wilson, 2004; Navarre-Sitchler et al., 2013).

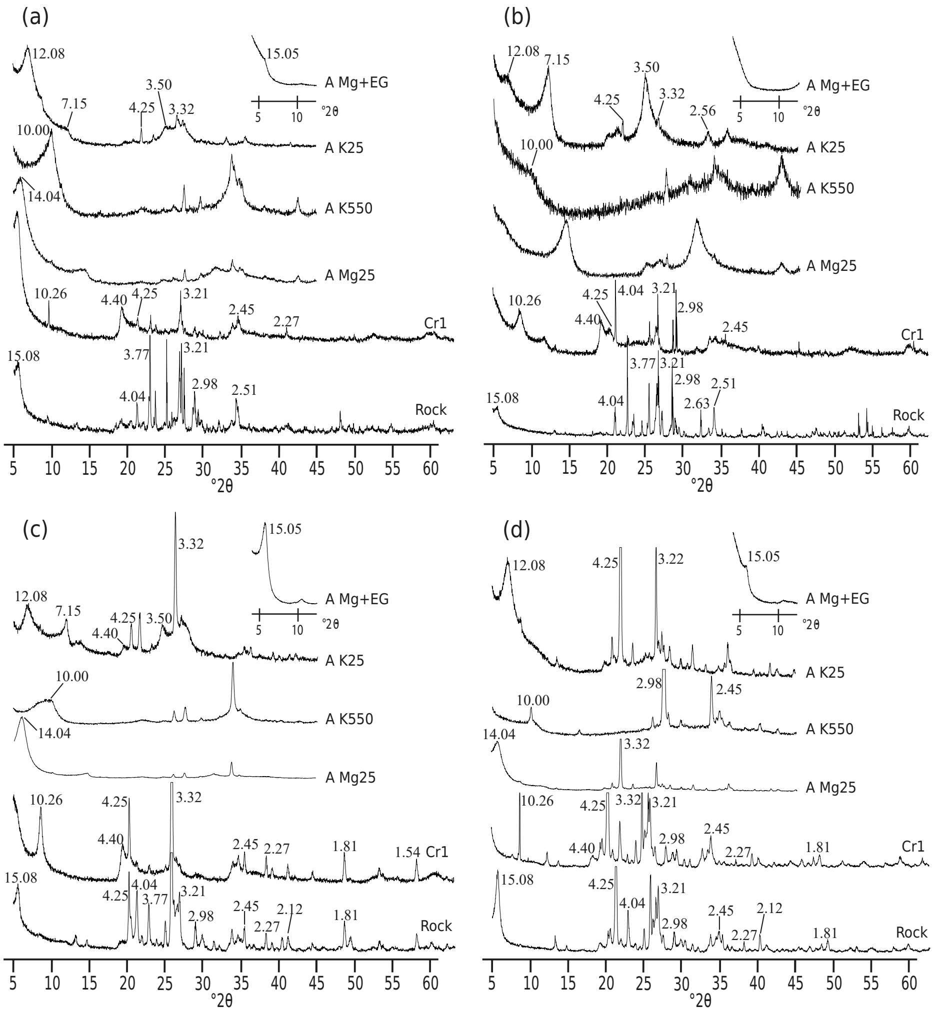

Figure 3. X-ray diffractograms (CuKalpha) of samples from horizon A (clay), Cr (saprolite) and RCr (rock) of P1 (a), P4 (b), P5 (c) and P7 (d). Interplanar space in Angstrom (Å).

The four profiles derived from basic rocks (P1, P2, P3 and P4 - Table 2) are located at an altitude between 218 and 284 m, while the other four profiles from acidic rocks (P5, P6, P7 and P8) are arranged at an altitude superior and 425 m, belonging, respectively, to the 1st flow (basalt/andesite –120 million years) and 4th flow (rhyolith) described by Sartori et al. (1975) in the region of Santa Maria, RS. The acidic and basic character of the source material did not result in a mineralogical differentiation of the solum, nor did it affect the physico-hydric characteristics of the evaluated Regosols.

Our results show the saprolite (Cr horizon) derived from volcanic rocks is an important portion of the soil due to its high water-holding capacity and AW for plant support. When associated with Regosols, the saprolite approximates the hydraulic behavior of the surface (A horizon) and interacts with plant roots, performing essential environmental services for ecosystem maintenance (Pedron et al., 2009). When close to the surface, likely in the Regosols, saprolites are clearly fragile in relation to contamination, so their identification, characterization and study is essential for sustainable land use planning (Santos et al., 2019).

CONCLUSIONS

Soil saturated hydraulic conductivity was considered low and without significant difference between A and Cr horizons. Total porosity was high, with most samples above 0.50 $m^3 m^{-3}$. Field capacity was higher in Cr than in A horizons in six of the eight evaluated profiles. Available water was higher in the Cr horizon than in A horizon in five soil profiles. There was no distinction in hydraulic properties of samples derived from acidic and basic rocks. Although the saprolite samples showed different mineralogical compositions, there was no significant difference in the mineralogical composition of the solum (horizon A). Mineralogical alteration in the Cr horizons (dissolution of mafic minerals and feldspars and precipitation of vermiculite and kaolinite) is responsible for the expansion of the porous matrix of the saprolite.

DATA AVAILABILITY

The data will be provided upon request.

FUNDING

This study was financially supported by the National Council for Scientifc and Technological Development - CNPq (Process No. 475874/2010-2) and the Research Support Foundation of Rio Grande do Sul - FAPERGS (Process No. 0904846).

AUTHOR CONTRIBUTIONS

Conceptualization: Fabrício de Araújo Pedron (lead) and Gabriel Antônio Deobald (equal).

Data curation: Fabrício de Araújo Pedron (lead).

Formal analysis: Alice Prates Bisso Dambroz (equal), Fabrício de Araújo Pedron (equal), Gabriel Antônio Deobald (equal) and Luís Antônio Coutrim dos Santos (equal).

Investigation: Alice Prates Bisso Dambroz (equal), Antônio Carlos de Azevedo (equal), Fabrício de Araújo Pedron (equal), Gabriel Antônio Deobald (equal), José Miguel Reichert (equal), Luís Antônio Coutrim dos Santos (equal) and Paulo Ivonir Gubiani (equal).

Methodology: Fabrício de Araújo Pedron (equal), Gabriel Antônio Deobald (equal), Luís Antônio Coutrim dos Santos (equal) and Paulo Ivonir Gubiani (equal).

Project administration: Fabrício de Araújo Pedron (lead).

Writing – original draft: Alice Prates Bisso Dambroz (equal), Antônio Carlos de Azevedo (equal), Fabrício de Araújo Pedron (lead), Gabriel Antônio Deobald (equal), José Miguel Reichert (equal), Luís Antônio Coutrim dos Santos (equal) and Paulo Ivonir Gubiani (equal).

Writing – review & editing: Alice Prates Bisso Dambroz (equal), Antônio Carlos de Azevedo (equal), Fabrício de Araújo Pedron (equal), Gabriel Antônio Deobald (equal), José Miguel Reichert (equal), Luís Antônio Coutrim dos Santos (equal) and Paulo Ivonir Gubiani (equal).

REFERENCES

Buhrke VE, Jenkins R, Smith DK. A practical guide for the preparation of specimens for X-ray fluorescence and X-ray diffraction analysis. New York: Wiley-VCH; 1998.

Costa ACS, Bigham JM, Tormena CA, Pintro JC. Clay mineralogy and cation exchange capacity of Brazilian soils from water contents determined by thermal analysis. Thermochim Acta. 2004;413:73-9. https://doi.org/10.1016/j.tca.2003.10.009

Elliott AC, Hynan LS. A SAS® macro implementation of a multiple comparison post hoc test for a Kruskal-Wallis analysis. Comput Meth Prog Bio. 2011;102:75-80. https://doi.org/10.1016/j.cmpb.2010.11.002

Fachi SM, Gubiani PI, Pedron FA, Rauber LR. Rocksoil skeleton increases water infiltration. Rev Bras Cienc Solo. 2023;47:e0230029. https://doi.org/10.36783/18069657rbcs20230029

Goldstein JI, Newbury DE, Michael JR, Ritchie NWN, Scott JHJ, Joy DC. Scanning electron microscopy and X-ray microanalysis. 2nd ed. New York: Plenum Press; 1992.

Gubiani PI, Albuquerque JA, Reinert DJ, Reichert JM. Tensão e extração de água em mesa de tensão e coluna de areia, em dois solos com elevada densidade. Cienc Rural. 2009;39:2535-8. https://doi.org/10.1590/S0103-84782009005000199

Gubiani PI, Reichert JM, Campbell C, Reinert DJ, Gelain NS. Assessing errors and accuracy in dew-point potentiometer and pressure plate extractor measurements. Soil Sci Soc Am J. 2012;77:19-24. https://doi.org/10.2136/sssaj2012.0024

Hasenmueller EA, Gub X, Weitzman JN, Adams TS, Stinchcomb GE, Eissenstat DM, Drohan PJ, Brantley SL, Kaye JP. Weathering of rock to regolith: The activity of deep roots in bedrock fractures. Geoderma. 2017;300:11-31. https://doi.org/10.1016/j.geoderma.2017.03.020

Holthusen D, Brandt AA, Reichert JM, Horn R. Soil porosity, permeability and static and dynamic strength parameters under native forest/grassland compared to no-tillage cropping. Soil Till Res. 2018;177:113-24. https://doi.org/10.1016/j.still.2017.12.003

Hubbert KR, Beyers JL, Graham RC. Roles of weathered bedrock and soil in seasonal water relations of *Pinus jeffreyi* and *Arctostaphylos patula*. Can J For Res. 2001;1:1947-57. https://doi.org/10.1139/cjfr-31-11-1947

IUSS Working Group WRB. World reference base for soil resources. International soil classification system for naming soils and creating legends for soil maps. 4th ed. Vienna, Austria: International Union of Soil Sciences (IUSS); 2022.

Klein VA, Reichert JM, Reinert DJ. Available water in a clayey Oxisol and physiological wilting of crops. Rev Bras Eng Agr Amb. 2006;10:646-50. https://doi.org/10.1590/S1415-43662006000300016

Maluf JRT. Nova classificação climática do Estado do Rio Grande do Sul. Rev Bras Agrometeorol. 2000;8:141-50.

Mehra OP, Jackson ML. Iron oxide removal from soils and clays by a dithionite-citrate system buffered with sodium bicarbonate. Clays Clay Miner. 1960;7:317-27. https://doi.org/10.1016/B978-0-08-009235-5.50026-7

Mesquita MGBF, Moraes SO. A dependência entre a condutividade hidráulica saturada e atributos físicos do solo. Cienc Rural. 2004;34:963-9. https://doi.org/10.1590/S0103-84782004000300052

Murphy CP. Thin section preparation of soils and sediments. Berkhamsted: AB Academic Pub; 1986.

Navarre-Sitchler AK, Cole DR, Rother G, Jin L, Bussf HL, Brantley SL. Porosity and surface area evolution during weathering of two igneous rocks. Geochim Cosmochim Acta. 2013;109:400-13. https://doi.org/10.1016/j.gca.2013.02.012

Pedron FA, Azevedo AC, Dalmolin RSD, Stürmer SLK, Menezes FP. Morphology and taxonomy classification of Neossolos and saprolites derived from volcanic rock of the Serra Geral formation in Rio Grande do Sul, Brazil. Rev Bras Cienc Solo. 2009;33:119-28. https://doi.org/10.1590/S0100-06832009000100013

Pedron FA, Azevedo AC, Dalmolin RSD. Mineral weathering in Neossolos in a climo-litosequence on the Rio Grande do Sul Plateau, Brazil. Cienc Rural. 2012;42:451-8. https://doi.org/10.1590/S0103-84782012000300011

Pedron FA, Fink JR, Dalmolin RSD, Azevedo AC. Morfologia dos contatos entre solo-saprolito-rocha em Neossolos derivados de arenitos da formação Caturrita no Rio Grande do Sul. Rev Bras Cienc Solo. 2010;34:1941-50. https://doi.org/10.1590/S0100-06832010000600019

Pedron FA, Fink JR, Rodrigues MF, Azevedo AC. Hydraulic conductivity and water retention in Leptosols-Regosols and saprolite derived from sandstone, Brazil. Rev Bras Cienc Solo. 2011;35:1253-62. https://doi.org/10.1590/S0100-06832011000400018

Pedron FA, Oliveira RB, Dalmolin RSD, Azevedo AC, Kilca RV. Boundary between soil and saprolite in Alisols in the South of Brazil. Rev Bras Cienc Solo. 2015;39:643-53. https://doi.org/10.1590/01000683rbcs20140229

Pereira CA, Mulazzani RP, van Lier QJ, Pedron FA, Gubiani PI. Particle arrangement and internal porosity of coarse fragments affect water retention in stony soils. Eur J Soil Sci. 2023;74:e13382. https://doi.org/10.1111/ejss.13382

Reichert JM, Albuquerque JA, Kaiser DR, Reinert DJ, Urach FL, Carlesso R. Estimation of water retention and availability in soils of Rio Grande do Sul. Rev Bras Cienc Solo. 2009b;33:1547-60. https://doi.org/10.1590/S0100-06832009000600004

Reichert JM, Cechin NF, Reinert DJ, Rodrigues MF, Suzuki LEAS. Ground-based harvesting operations of Pinus taeda affects structure and pore functioning of clay and sandy clay soils. Geoderma. 2018;331:38-49. https://doi.org/10.1016/j.geoderma.2018.06.012

Reichert JM, Rosa VT, Vogelmann ES, Rosa DP, Horn R, Reinert DJ, Sattler A, Denardin JE. Conceptual framework for capacity and intensity physical soil properties affected by short and long-term (14 years) continuous no-tillage and controlled traffic. Soil Till Res. 2016;158:123-36. https://doi.org/10.1016/j.still.2015.11.010

Reichert JM, Suzuki LEAS, Reinert DJ, Horn R, Håkansson I. Reference bulk density and critical degree-of-compactness for no-till crop production in subtropical highly weathered soils. Soil Till Res. 2009a;102:242-54. https://doi.org/10.1016/j.still.2008.07.002

Reinert DJ, Albuquerque JA, Reichert JM, Aita C, Andrada MMC. Limites críticos de densidade do solo para o crescimento de raízes de plantas de cobertura em Argissolo Vermelho. Rev Bras Cienc Solo. 2008;32:1805-16. https://doi.org/10.1590/S0100-06832008000500002

Rose KL, Graham RC, Parker DR. Water source utilization by *Pinus jeffreyi* and *Arctostaphylos patula* on thin soils over bedrock. Oecologia. 2003;134:46-54. https://doi.org/10.1007/s00442-002-1084-4

Santos HG, Jacomine PKT, Anjos LHC, Oliveira VA, Lumbreras JF, Coelho MR, Almeida JA, Araújo Filho JC, Oliveira JB, Cunha TJF. Sistema brasileiro de classificação de solos. 5. ed. rev. ampl. Brasília, DF: Embrapa; 2018a.

Santos JCB, Le Pera E, Souza Júnior VS, Corrêa MM, Azevedo AC. Gneiss saprolite weathering and soil genesis along an east-west regolith sequence (NE Brazil). Catena. 2017;150:279-90. https://doi.org/10.1016/j.catena.2016.11.031

Santos JCB, Le Pera E, Souza Júnior VS, Oliveira CS, Juilleret J, Corrêa MM, Azevedo AC. Porosity and genesis of clay in gneiss saprolites: The relevance of saprolithology to whole regolith pedology. Geoderma. 2018b;319:1-13. https://doi.org/10.1016/j.geoderma.2017.12.031

Santos RA, Sermarini RA, Guerra AR, Santos JCB, Azevedo AC. Field perception of the boundary between soil and saprolite by pedologists and its differentiation using mathematical models. Rev Bras Cienc Solo. 2019;43:e0180104. https://doi.org/10.1590/18069657rbcs20180104

Santos RD, Santos HG, Ker JC, Anjos LHC, Shimizu SH. Manual de descrição e coleta de solo no campo. 7. ed. rev. ampl. Viçosa, MG: Sociedade Brasileira de Ciência do Solo; 2015.

Sartori PL, Maciel Filho C, Menegotto E. Contribuição ao estudo das rochas vulcânicas da Bacia do Paraná na região de Santa Maria, RS. Rev Bras Geocienc. 1975;5:141-59.

Soil Survey Staff. Keys to soil taxonomy. 13th ed. Washington, DC: United States Department of Agriculture, Natural Resources Conservation Service; 2022.

Soil Survey Staff. Soil survey manual. Washington, DC: United States Department of Agriculture, Natural Resources Conservation Service; 2017. (Agricultural Handbook, 18).

Stolf R. Teoria e teste experimental de fórmulas de transformação dos dados de penetrômetro de impacto em resistência do solo. Rev Bras Cienc Solo. 1991;5:229-35.

Streck EV, Kämpf N, Dalmolin RSD, Klamt E, Nascimento PC, Giasson E, Pinto LFS. Solos do Rio Grande do Sul. 3. ed. Porto Alegre: Emater/RS, Ascar; 2018.

Stürmer SLK, Dalmolin RSD, Azevedo AC, Pedron FA, Menezes FP. Relação da granulometria do solo e morfologia do saprolito com a infiltração de água em Neossolos Regolíticos do rebordo do Planalto do Rio Grande do Sul. Cienc Rural. 2009;39:2057-64. https://doi.org/10.1590/S0103-84782009005000141

Teixeira PC, Donagemma GK, Fontana A, Teixeira WG. Manual de métodos de análise de solo. 3. ed. rev e ampl. Brasília, DF: Embrapa; 2017.

Vepraskas MJ. Predicting contaminant transport along quartz veins above the water table in a mica-schist saprolite. Geoderma. 2005;12647-57. https://doi.org/10.1016/j.geoderma.2004.11.006

Wald JA, Graham RC, Schoeneberger PJ. Distribution and properties of soft weathered bedrock at ≤ 1 m depth in the contiguous United States. Earth Surf Process Landf. 2013;38:614-26. https://doi.org/10.1002/esp.3343

Whitting LD, Allardice WR. X-ray diffraction techniques. In: Klute A, editor. Methods of soil analysis: Part 1 Physical and mineralogical methods. Madison: American Society of Agronomy, Soil Science Society of America; 1986. p. 331-62.

Wilson MJ. Weathering of the primary rock-forming minerals: Processes, products and rates. Clay Miner. 2004;39:233-66. https://doi.org/10.1180/0009855043930133

Yeomans JC, Bremner JM. A rapid and precise method routine determination of organic carbon in soil. Commun Soil Sci Plant Anal. 1988;19:1467-76. https://doi.org/10.1080/00103628809368027

Zhang YW, Wang KB, Wang J, Liu C, Shangguan ZP. Changes in soil water holding capacity and water availability following vegetation restoration on the Chinese Loess Plateau. Sci Rep. 2021;11:9692. https://doi.org/10.1038/s41598-021-88914-0